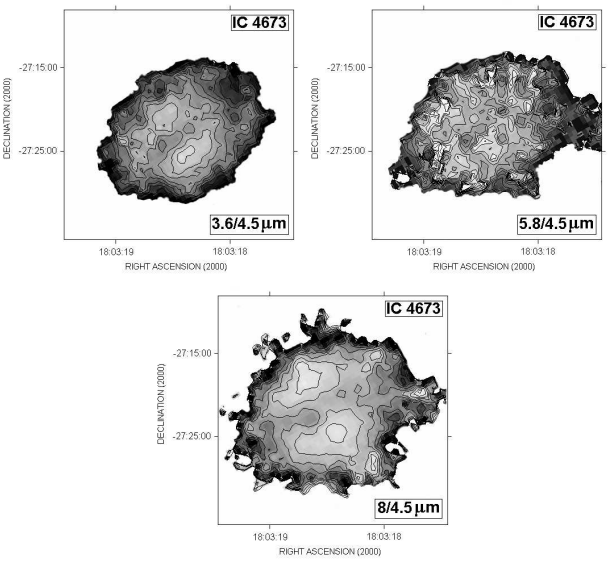

Fig. 8. IRAC band ratio mapping for IC 4673, where the parameters [D, E] are given by [0.2, 0.0865] for 3.6 μm/4.5 μm, [0.2, 0.0777] for 5.8 μm/4.5 μm, and [1.7, 0.0943] for 8.0 μm/4.5 μm. The structure of the 5.8 μm/4.5 μm map is highly complex, and shows little evidence for systematic changes with position in the shell. The 3.6 μm/4.5 μm and 8.0 μm/4.5 μm maps, on the other hand, show evidence for ratio minima along the minor axis of the source, at the positions of maximum surface brightness.

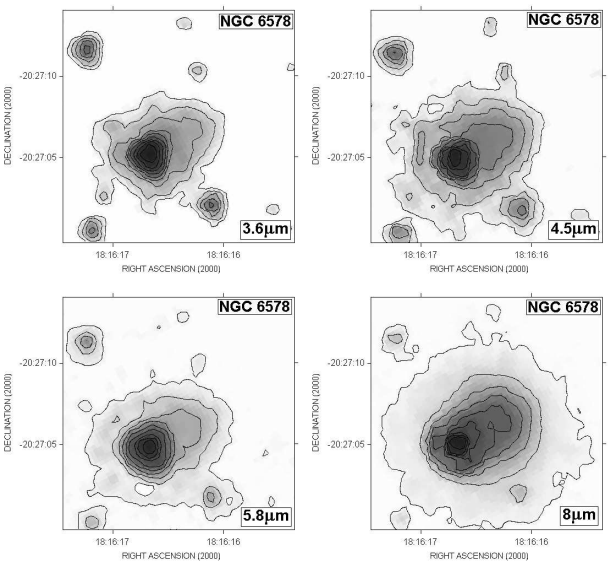

Fig. 9. IRAC contour mapping of NGC 6578, where parameters [A, B, C] are given by [11, 2.56, 0.2680] at 3.6 μm, [6, 1.56, 0.3051] at 4.5 μm, [12.5, 6.50, 0.2513] at 5.8 μm, and [25, 19.67, 0.1947] at 8.0 μm. The map shows evidence for a bright interior elliptical shell, and a more circular halo at longer wavelengths. The point source close to $\alpha = 18^h16^m16^s.65$, $\delta = -20°27'04''.7$ is likely to correspond to an unrelated field star.

3.3. *NGC 6578*

NGC 6578 has an elliptical shell with dimensions $\cong 7.5 \times 25$ arcsec^2 (see e.g., the imaging of Corradi et al. (2003), and the HST [OIII] image illustrated by Hajian et al. (2007), surrounded by an irregular outer halo with size 14×60 arcsec^2 (Corradi et al. 2003). Modelling of the spectral lines in the source has been undertaken by Hajian et al. (2007), whilst Perinotto et al. (1994) determine abundance ratios He/H $\cong$ 0.14, N/O $\cong$ 0.2; values which are also similar to those estimated by Perinotto, Morbidelli, & Scatarzi (2004) (He/H $\cong$ 0.198, N/O $\cong$ 0.21). It would therefore appear that whilst the helium abundance is high, the nebula is not a Type I source.

The mapping in Figure 9 doesn't bear much relation to the symmetric structure noted in the visible, partially because of the presence of a bright point source close to $\alpha = 18^h16^m16^s.65$, $\delta = -20°27'04''.7$. It is possible that this corresponds to a rather red (peaking at $\lambda \sim 6$ μm) background object which is unrelated to NGC 6578, and is appreciably contaminating the inner source structure.

We have therefore attempted to side-step this feature in our profiles in Figure 10, where it is clear that trends in all of the channels are very much the same. This results in relatively modest variations in the IRAC band ratios (Figure 10, lower panel), although there is some evidence for peaks in 5.8 μm/4.5 μm and 8.0 μm/4.5 μm close to the limits of the interior shell (i.e. at relative positions $\pm$5 arcsec). It is fascinating to note that the visual halo about the source has its counterpart at 8.0 μm as well, where we see evidence for a circular region with size 11×12 arcsec^2. This is, in fact, a lower limit dimension, and profiles show that the halo extends to distances of at least $\sim$17 arcsec from the centre.

Such a result is somewhat surprising, given the weakness of the halo in the visible. Corradi et al. (2003) find that the halo trends for H + [NII] and [OIII] are very closely similar, and imply intensities of $\sim$0.15 at RP = 5 arcsec, $\sim 5 \times 10^{-3}$ at 10 arcsec, and $\sim 10^{-3}$ at 20 arcsec when compared to peak strengths within the nucleus of the source. This is well below what would ordinarily be detectable with *Spitzer*. The reason why we are detecting the halo in the present observations is because it is relatively very much brighter in the MIR, and has a relative intensity $\sim 2 \times 10^{-2}$ at distances of 15 arcsec from the centre.